APPLICATION OF IMPOSED MOTION METHOD FOR MODEL FLUTTER TESTS IN HIGH-SPEED WIND TUNNELS

Boris D. Bryantsev

TsAGI, Zhukovsky, RUSSIA
brbd@progtech.ru

Keywords: aeroelasticity, flutter, frequency response functions, wind tunnel.

Abstract: A brief background on Frequency Response Functions (FRFs) measurement technology applied to mechanical systems on the basis of imposed motion method (kinematic excitation method) is presented herein. Shown is the possibility to use analysis to evaluate an effect of adding extra concentrated mass, stiffness and damping, in the points of application of driving forces, on the FRFs of a tested article with use of experimental FRFs of initial unmodified structure as a reference. The capabilities of the technology for flutter research are demonstrated by the example of GVT of a dynamically-scaled model of an all-movable stabilizer intended for flutter wind tunnel tests, with an electro hydraulic actuator used to impose model displacement in the driving point. The test techniques, as well as details of measuring FRFs under wind tunnel flow conditions with the use of specific multi-sine test signal for structure excitation are described. Presented are examples of measured in-flow model FRFs, and identified modal data as a function of flow parameters, including eigenfrequencies, eigendamping and eigenmodes recovered for unmodified model (free of the links imposed by the actuator) at flow speed beyond flutter boundary.

1 INTRODUCTION

. The method of imposed motion in structural dynamics, or, in other words, the method of kinematic excitation is described in [1,2]. The idea of the method may be presented as follows: let us consider an elastic article under test (Fig.1), which structural pure sine oscillations may be measured as a set of complex amplitudes $X_i(j\omega)$ in the points $i=1,\ldots,n$ by a set of n sensors. For instance, this may be dynamically scaled model for wind tunnel (WT) flutter tests. According to [1,2], such a flutter test model is mounted on movable supports, e.g. on the top of the rods of hydraulic actuators (HA1, HA2) supplied with force cells to measure the forces $f_i(j\omega)$ occurred between the rods and the model.

The goal is to determine characteristics of dynamic performance of "free" unsupported model on the basis of measurements on the model being supported. Providing an assigned sine motion of the rods $X_{fi}(j\omega)$ at given frequencies and measuring model oscillations $X_i(j\omega)$ and the forces $f_i(j\omega)$, it is possible to get the FRF matrix containing model FRFs $W_{ij}(j\omega)=X_i(j\omega)/f_j(j\omega)$, including those in wind tunnel flow. By definition, $W_{ij}(j\omega)$ is the response of the sensor number i to the unit force number j: $f_j(j\omega)=1$, while all other forces are zero. This means $W_{ij}(j\omega)$ is the FRF matrix of the unsupported model free of the restraints imposed by the rods. Using the results of measuring $W_{ij}(j\omega)$ at various ω at different air flow speed, it is possible to determine frequencies and logarithmic decrements of in-flow elastic vibration modes of the "free" model, and finally, to determine its flutter speed.

According to [1,2], motion of the supports may be provided by means of electro-hydraulic actuators that realize "rigid" excitation. In this case, motion of the model in the points of connection with the supports (actuator rods) is governed by actuator drive signals, i.e. imposed motion, or kinematic excitation is provided. Model structural dymanics in flow, without excitation, corresponds to the case with fixed supports. The envelope of the flow parameters that is free of flutter for the supported model, may completely contain the envelope free of flutter of the unsupported model, or may be essentially wider than the latter. In this case, using virtually direct measurements, the dynamic characteristics of the unsupported model may be determined not only within its flutter boundaries, but also beyond them.

Application of the above techniques in daily practice in the time of the publications [1,2] was not rational as no techniques of matrix FRF measurements within the acceptable time were available at that period. Today, thanks to the wide use of high performance digital multi-channel PC-based data acquisition, processing and control systems, these problems are practically solved. Moreover, use of multi-sine drive signals allows FRF to be measured within very short periods of time. Thus the ideas formulated in [1,2] became of practical value for flutter tests. In particular, modal analysis on the basis of measured vector FRFs has become an ordinary working tool.

The basic elements of modal analysis and flutter prediction based on subcritical (below flutter boundary) measurements are described in [3,4,5]. Appropriate in-house TsAGI software allow modal analysis and flutter prediction of a flexible aircraft to be carried out on the basis of identification of differential equations of structural dynamics in the presence of air flow.

The measured responses to the following types of excitation can be used:

- pure sine,
- multi-sine of a specific waveform,
- controlled pulse excitation,
- uncontrolled pulse excitation,
- external uncontrolled random excitation (close to "white noise").

The Polymax modal analysis algorithm [6] used in "LMS Test. Lab – Structural testing" [7] almost coincides with the modal identification procedures described in [4,5].

Also, the techniques described in [1,2] enable the effect of extra links (restraints) imposed onto the tested article in the driving point to be evaluated without complicated analysis. For simplicity, let us consider single input/multiple output excitation (SIMO). Consider a linear dynamic system (Fig.2) under pure sine excitation by the force $f(j\omega)$ applied in a driving point. System displacements are measured in the driving point $X_f(j\omega)$ and other output points $X_i(j\omega)$, $i=1,\ldots,n$. Let the vector FRF $W^T(j\omega)=\{W_1(j\omega),\ldots,W_n(j\omega)\}$, where $W_i(j\omega)=X_i(j\omega)/f(j\omega)$, be measured. Consider also an additional linear dynamic system connected to the tested article in the driving point in parallel to the source of excitation. Let the dynamic stiffness of the additional system be $Q(j\omega)$. It is easily shown then that the components of the vector FRF of the tested article with the connected additional system is calculated by the formula:

$$\tilde{W}_i(j\omega)=\frac{W_i(j\omega)}{1+Q(j\omega)*W_f(j\omega)},$$

where $W_f(j\omega)=X_f(j\omega)/f(j\omega)$ is the component of the vector FRF of the initial tested article in the driving point. Particularly, when the additional system is a spring with stiffness K, then its dynamic stiffness $Q(j\omega)=K$; when the additional system is a damper, then $Q(j\omega)=j\omega D$, where

D is the damping coefficient; when the additional system is a weight with mass M, then $Q(j\omega)=-\omega^2 M$. The simultaneously connected mass, damper and spring gives the dynamic stiffness $Q(j\omega)= -\omega^2 M+K+j\omega K$. Once FRFs of the initial tested article are measured, then FRF of the article modified by adding extra mass, stiffness and damping in the driving point may be obtained by simple recalculation.

This paper describes the basic elements of structural dynamics testing techniques with use of kinematic excitation, or imposed motion method. The efficiency is shown on the example of flutter tests of an elastically scaled model of all-movable stabilizer in transonic T-128 wind tunnel.

2 EXPERIMENTAL RIG AND TEST TECHNOLOGY

The model was tested on a dedicated test rig mounted on the floor of the T-128 test-section (fig.3). The model was mounted on a vertical rotating shaft supported by the upper and lower bearings. The bending of the shaft between the upper and lower bearings provides modeling of full-scale root stiffness in bending.

The shaft is instrumented with strain gauges: out-of plane bending (T2) and in-plane (chordwise) bending (T4). The rotation root stiffness is modeled with two flat springs, one of which is instrumented with strain gauge T3 to measure the rotation angle of the model root rib. To provide model forced oscillations in tunnel air flow, the rig is equipped with a small-size electrohydraulic actuator.

The actuator driving cylinder is fixed on the model in the nose area of the root rib.

To monitor model oscillations and excitation system performance, an accelerometer D1 and the rod position feedback sensor T1 are installed. The actuator rod is connected to the free end of a short cantilevered beam K1 via a flexible link T. The beam K1 is additionally supported by struts K2 and K3 attached to the rig fairing. A strain-gauge-based force cell to measure the excitation force is mounted between the cantilevered beam/struts junction and a flexible link.

The stabilizer plane itself is instrumented with two strain-gauge half-bridges T5 and T6 to measure elastic deformations of the plane. The above listed sensors provide the so-called “flight system of sensors” (FSS) used for measurements in tunnel flow.

Dedicated calibration tests at zero flow speed have been performed to determine the correspondence between FSS outputs and model displacements in the set of nodal control points. During the calibration tests model forced oscillations have been detected both by FSS sensors and nodal accelerometers. The nodal grid on the plane is shown in Fig.4. The transition matrix from FSS outputs to nodal control point displacements has been generated on the basis of the calibration results.

The control of excitation, signal sampling, data acquisition and preliminary analysis, identification of mathematical models and analysis of flutter performance on the basis of experimental data are provided by the dedicated PC-based multichannel data acquisition system of TsAGI in-house development. The system block-diagram is shown in Fig.5. The excitation (drive) signal Ugen with assigned spectral and amplitude features is built up in digital domain by a special software module and outputted through the digital-to-analog converter (DAC) to the actuator control unit as a target signal.

There it is summed up with an inverse feedback sensor signal provided by the strain gauge T1 and appropriate amplifiers. The mismatch between the target and feedback signals is transmitted to the servo valve to control the position of the actuator rod. The D1 accelerometer signal, via a charge amplifier, is sampled by an analog-to-digitial converter (ADC). Signals of the following sensors are sampled by ADCs via stain gauge conditioning amplifiers: force cell F, rod position feed-back sensor T1 and strain gauges T2,…,T6 to measure model elastic oscillations in the tunnel flow.

During each test (tunnel run), sensor signals are acquired at pre-selected tunnel flow conditions (test steps) under multi-sine model excitation over the frequency range of the first five vibration modes (10-140 Hz). Measurement duration at each step is 20-60 seconds. Number of steps in each test is determined by technological capabilities of the WT.

For instance, a fragment of model oscillation waveforms within 8 seconds under multisine excitation in flow at M=1.4, Q = 20 300 kN/m^2 is shown in Fig.6. The lower curve in Fig.6 is for the feed-back sensor T1. Other curves as go from the top to the bottom are for T2,…,T7, F, D1 and Ugen signals accordingly.

Signal spectra and vector FRFs are calculated then between tunnel runs on the basis of these time-domain signals. For example, the spectra of the drive signal Ugen, force cell F and shaft bending T2 signals are shown in Fig.7. Fig. 7 demonstrates rather a complicated spectrum profile of the "generator" signal. It was selected so both to provide reliable excitation of all the modes of interest, and from the other hand, not to cause too high oscillations in the vicinity of resonance frequencies of the model with excitation system connected. Specific dips in the vicinity of frequencies of about 19, 32, 85 and 125 Hz can be well seen in force cell spectrum under locally constant profile of the drive signal. Such dips are generic for kinematic excitation method.

Figs. 8a, 8b show typical magnitude and phase FRFs obtained with multisine excitation in flow at M=1.4, Q=20 300 N/m^2. In these figures the patterns of magnitude and phase variation versus frequency typical for main vibration modes can be well seen.

Vector FRFs measured in flow is the initial source to obtain in-flow modal data (frequencies, logarithmic decrements and complex vibration eigen modes). Figures 9a,9b show dependence of eigenfrequencies (f1,…,f5) and decrements (d1,…,d5) on dynamic pressure for the first five vibration modes obtained by in-flow measurements at atmospheric pressure in the WT staganation chamber. Additionally, dynamic pressure versus Mach number (M) is shown in fig. 9a. Note that all the data presented in these figures have been obtained during as little as two short WT runs. The data in these figures provide clear visual indication of typical errors in evaluation of model frequencies and decrements in flow.

Note that measurements at M=1.0 (at maximum dynamic pressure) were made within flutter envelope of the unsupported free model. This became possible due to the fact that flutter boundary of the supported model (with hydraulic excitation system connected) is far beyond than that for the free model.

The real and imaginary parts of the eigenvector for the first (unstable) vibration mode in flow at q = 37 000 N/m^2 and M=1.0 is shown in Fig. 10a, 10b as the mode shape in nodal control points. One can see from the figures that the imaginary part of the eigenvector is essentially less than the real one. For other modes, relative value of an imaginary part is even less, so only real parts of the 3rd , 4th , and 5th mode eigenvectors in flow are shown in

Figs.10c,10d,and 10e. The second mode is model in-plane oscillations as a rigid body; it just rotates chordwise about the point of the shaft/root rib intersection.

3 CONCLUSION

The above data distinctly show that the method of imposed motion (kinematic excitation) in model wind tunnel flutter researches can be effective and reliable technique to ensure tests within short time with minimum risk of model failure due to flutter.

The method and relevant technology can be recommended for broad practical application in model wind tunnel flutter researches.

4 REFERENCES

[1] Strelkov S.P. “Substantiation of method of experimental determination of oscillatory instability of a linear discrete system (method of "set" oscillatory of displacements)” *Collected papers of TsAGI Num. 2200 « Dynamic Problems of Aeroelasticity » the Collection of papers devoted to the memory of S.P.Strelkov.* TsAGI Publishing department, Moscow, 1983. (in Russian)

[2] Asher G.W., Hyland F.G. “The use of admittance techniques in dynamic model testing” *AIAA Symposium of Structural Dynamics and Aeroelasticity.* New York, 1965.

[3] Dat R., Meurzec J.L. “Exploitation par Lissage Mathematigue des Mesures d'Admittance d'un Systeme Linearise”. - *La Recherce Aerospatiale.* no.1972-4 (septembre 1972).

[4] Bryantsev B.D. "Base Algorithms of Identification and Correction of Mathematical Models of Structure Dynamics of Flight Vehicles by Results of Dynamic Tests”, preprint TsAGI N7, Moscow, 1990.(in Russian)

[5] Bryantsev B.D., Kloukin N.G., Paryshev S.E., Zichencov M.Ch. “Modal Parameters Identification and Flutter Prediction From Turbulence - Excited Responses” *V International Symposium Proceedings “New aviation technologies of the XXI century”* Zhukovsky, Moscow Region, Russia, 1999

[6] Bart Peetersa, Herman Van der Auweraera, Patrick Guillaumeb and Jan Leuridana “The PolyMAX frequency-domain method: a new standard for modal parameter estimation” *IOS Press, Shock and Vibration 11* (2004) 395-409

[7] LMS INTERNATIONAL, LMS Test. Lab **-** Modal Analysis and Operational Modal Analysis Rev 5A. Leuven, Belgium, www.lmsintl.com, 2004.

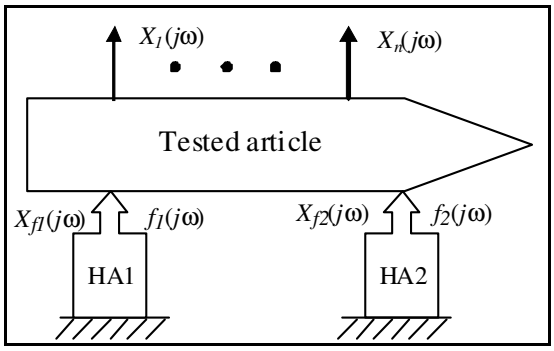

Figure 1: Outline of test method set movements

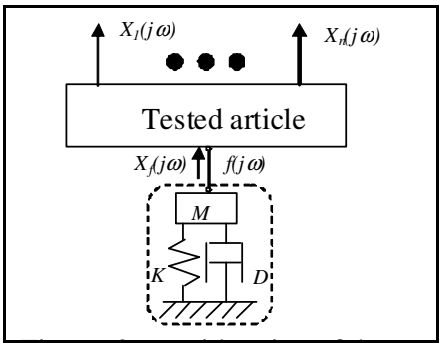

Figure 2: Consideration of the additional links

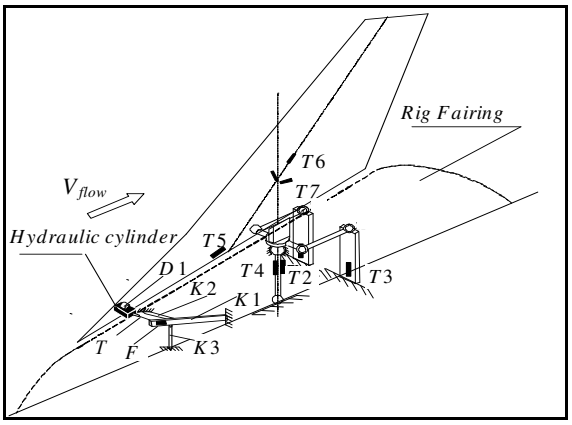

Figure 3:

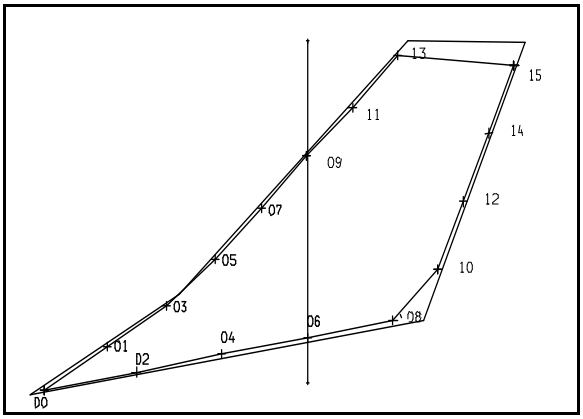

Figure 4: GVT nodal points

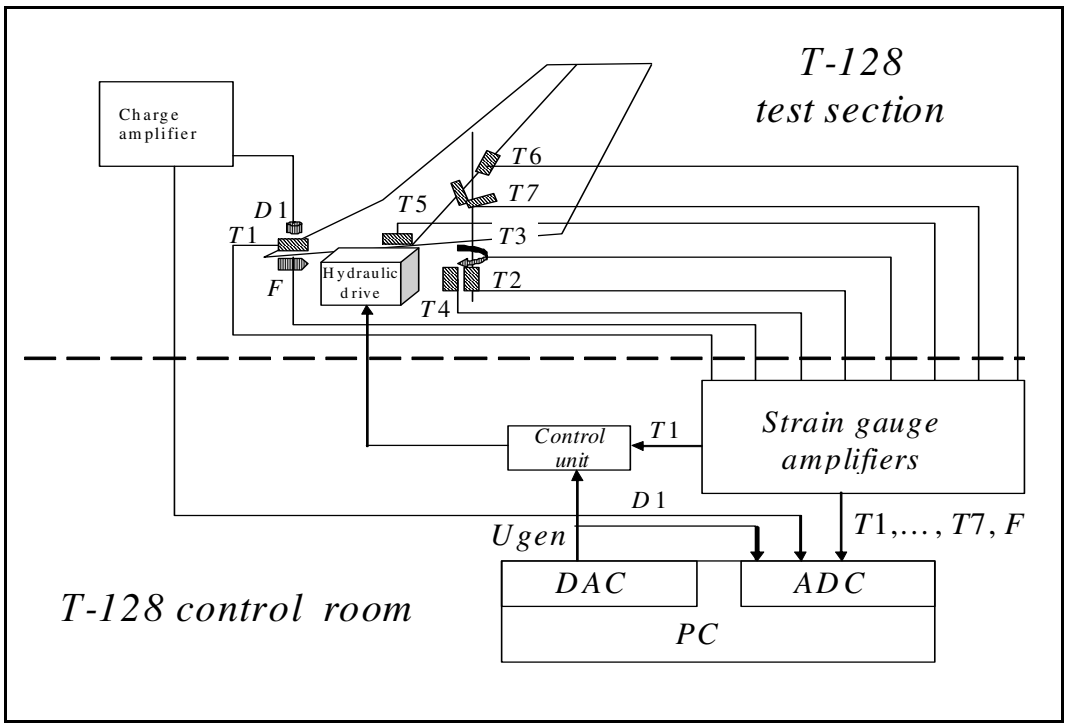

Figure 5: Data acquisition and control system

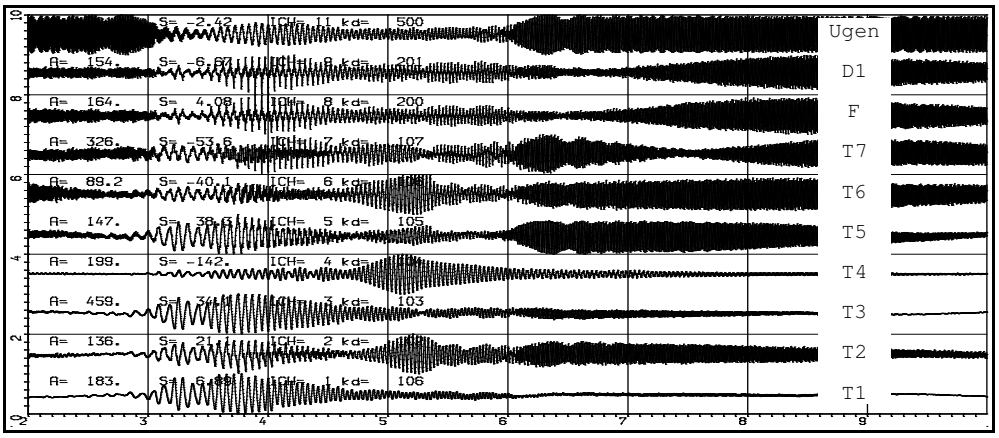

Figure 6: An example of model oscillations in flow at M=1.4, Q=20 300 N/m^2

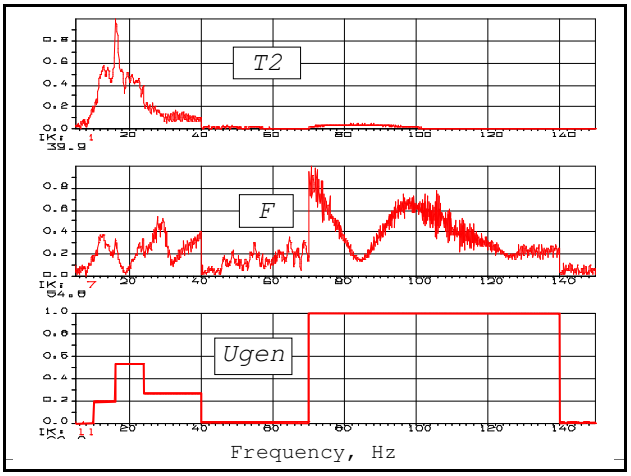

Figure 7: Signal spectra for "generator" Ugen, force cell F and shaft bending T2

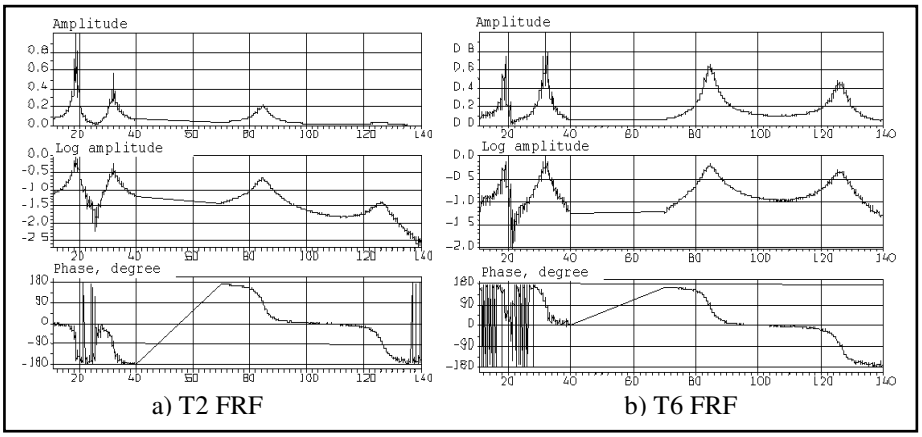

Figure 8: FRF components in flow at M=1.4, Q=20 300 N/m^2

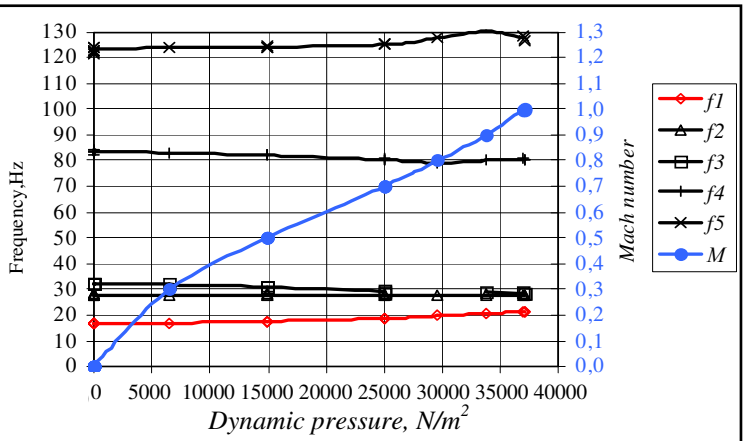

a) Model eigenfrequencies and Mach number vs. dynamic pressure at standard T-128 flow conditions

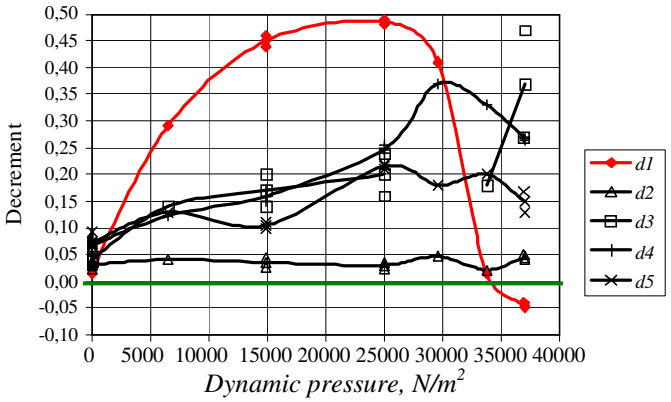

b) Decrements vs. dynamic pressure at standard T-128 flow conditions

Figure 9

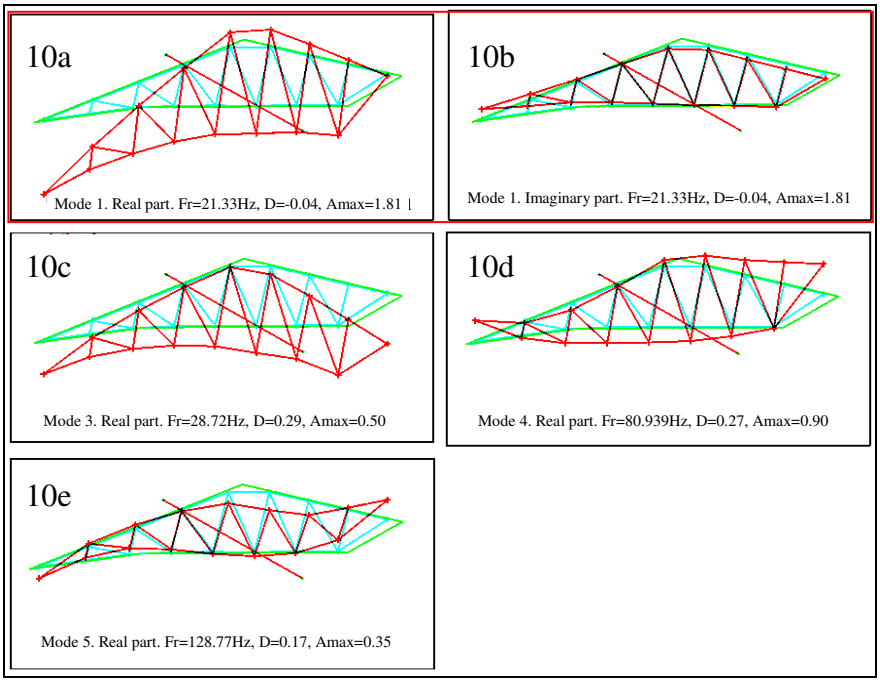

Figure 10: Model eigenvectors in flow at q = 37 000 N/m^2 and M=1.0